J. M. Martínez · H. Amarís · J. Sanz

Frequency domain modelling of random wound motor windings for insulation stress analysis

Abstract The use of conventional low voltage induction motors fed by pulse width modulated (PWM) inverters has begun to present important problems. These waveforms consist of steep-fronted pulses having very short rise times (about 100 ns in modern IGBT bridges) and high frequency repetition rates (up to 20 kHz) whose immediate consequences are additional electrical stresses in an induction motor's insulation system. In this paper a frequency domain model for the analysis and characterization of the internal voltage distribution in random wound coils is presented. The model allows voltage prediction in time domain when an inverse fast Fourier transform (FFT) transformation is performed, and requires only a few frequency domain impedance measurements. This methodology will be useful for accurately predicting the voltage distribution in motor windings during the design stage, and reducing the risk of premature failure in motor insulation. Experimental and theoretical results are presented and compared and model effectiveness using different approximations is studied.

Keywords Frequency domain analysis · Time domain analysis · Random wound winding · Pulse width modulation · Steep-fronted transients · Voltage distribution

1 Introduction

In recent years there has been a lot of concern about insulation endurance in low voltage motors fed by variable-frequency pulse width modulated (PWM) drives. Electrical stresses in this type of insulation, originally designed to support sinusoidal voltages, are now of a very different nature, resulting in accelerated aging and a much shorter operating life. Modern inverters that use IGBT technology produce waveforms formed by very steep fronted square pulses, with very short rise times, ranging from tens to hundreds of nanoseconds, and a repetition rate of tens of kilohertz. When these pulses, which can be considered travelling waves, arrive at motor terminals, they are partly reflected and partly transmitted into the windings, due to the difference of the characteristic impedance of cable and motor winding. The resulting overvoltages, which can reach up to twice the dc voltage level in the inverter, and the short rise times cause a very uneven voltage distribution along the winding, and most of the voltage falls within the first coil of the winding [1–3]. Furthermore, there is an uneven voltage distribution within this first coil [4], with higher electrical stresses in the first turns [2, 3, 5] and last turns [2, 6]. In random wound windings this can be a problem because these turns can be in contact and the interturn voltage may exceed the partial discharge inception voltage (PDIV) of the winding insulation. Most of the published papers refer to interturn insulation as the weakest point [5, 7]. Besides, these steep and repetitive changes in voltage polarity can inject some trapped charge, thus degrading the operating conditions of the insulation. When all these factors combine together the result is an accelerated aging of the insulating materials and a shorter life for insulation systems [2, 8].

These reasons make it desirable from the early design stage to have an estimation of the overvoltages caused by inverter drives that can assure an adequate insulation for the stator winding. Moreover, voltage distribution prediction within the coils of a stator winding could be useful for characterizing electrical stresses and will allow the study of new insulation system designs in inverter fed machines.

Earlier studies on voltage distribution analysis were applied to form-wound high voltage motors. The

J. M. Martínez (✉) · H. Amarís · J. Sanz
Electrical Engineering Department,
University Carlos III de Madrid,
Leganés (Madrid), PO 28911, Spain
E mail: jmmtarif@ing.uc3m.es
Tel.: +34 91 6248852
Fax: +34 91 6249430
E mail: hamaris@ing.uc3m.es
E mail: jsanz@ing.uc3m.es

problem here was mainly the propagation of atmospheric surges through transformers to motor terminals or switching overvoltages produced by vacuum-interrupters. With this type of windings, multiconductor transmission line models were adopted [9, 10]. These models allowed a good voltage prediction at different winding positions for these non-repetitive surges, but the computation of the electrical parameters made use of a completely different procedure inapplicable to random-wound windings. Furthermore, rise times in these cases are always greater than 200 ns, so that this limited upper bandwidth allows manufacturer to propose different simplifications in these models (like neglecting losses and/or mutual inductances between turns) without loss of accuracy.

This paper presents a new methodology for modelling random wound windings in low voltage motors that permits analysis and prediction of voltage distribution along the winding when fed with PWM waveforms. The model, formulated in the frequency domain, is complete and easy to implement, and requires only a limited number of frequency domain measurements to experimentally determine all its parameters. The method has been outlined for easy implementation when designing motor windings thus allowing for an optimal life expectancy.

Modelling in the frequency domain has several advantages. One is that electrical parameters are of the same nature as those used in equivalent circuit calculations. The other most important advantage is that the frequency domain is the natural way to analyse dielectric properties of electrical insulating materials. As a consequence, the resulting equivalent circuit model also contains all the relevant information relative to material aging and polarisation mechanisms.

On the other hand, the system response is usually represented in the time domain, and inverse FFT algorithms are mandatory. This will add some extra complexity and computational load to our model.

2 Model description

Due to the high frequencies involved in the analysis (up to 9 MHz), each phase winding of the motor is represented by a distributed parameter line as depicted in Fig. 1. Every section of this line includes not only the series resistance R_i and inductance L_i of the windings, but also the stray capacitances between two consecutive elements and the stray capacitances between each winding element and ground. These two elements are represented as real capacitances, i.e., an ideal capacitor in parallel with a resistor representing dielectric losses (C_{ij} and R_{ij} for the turn-to-turn capacitance, and Ctg_i and Rtg_i for the turn-to-ground capacitance) to obtain enough accuracy [9, 11]. The model is completed with mutual inductances M between single elements. Due to the high number of turns in a practical winding, a single turn has been chosen as the single element of the model.

Input voltage is modelled as a sinusoidal voltage of 1 pu and variable frequency, applied between the input terminal and ground. The opposite terminal of the winding is left floating, representing the worst-case situation, because the pulse travelling wave is fully reflected at the end of the winding. When other phases are present, changes in the characteristic impedance are not so abrupt. In this configuration, the turn-to-ground insulation can be analysed. Temperature only affects the result through the variation of the coil resistance but has little influence on voltage distribution [12]. Nor does the model have to take into account the presence of the rotor, as demonstrated by some authors [9, 13].

The modelling- and analysing process comprises the following steps:

1. Impedance characterization in the frequency domain:

The impedance analyser computes complex impedance values using the quotient between the values

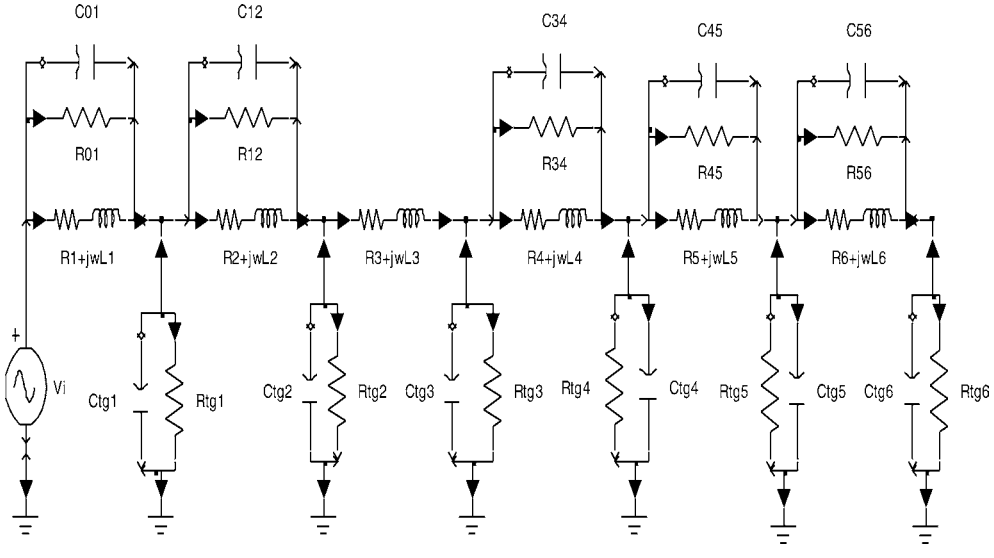

Fig. 1 Structure of the model

of measured voltage and injected current, at each frequency.

$Zt(\omega)$	Turn impedance
$Zm_{ij}(\omega)$	Inductive mutual impedance between turns#i and#j
$Ztt(\omega)$	Turn to turn impedance
$Ztg(\omega)$	Turn to ground impedance

2. Analytical solution

Once the impedance parameters are known, they are used in the analytical model in order to compute the nodal voltages in every node of interest. This solution can be achieved by applying mesh method to this equivalent circuit to get the current vector at every frequency $\boldsymbol{I}(\omega)=[I_1(\omega),\ I_2(\omega),\ I_3(\omega),\ I_4(\omega),\ I_5(\omega),\ I_6(\omega)]$ when a voltage signal is applied between the coil input and ground reference for each frequency component in the bandwidth of interest.

$$\begin{aligned} V_i(\omega) = {} & I_i(\omega)\cdot\lfloor Zt_i(\omega)+Ztg(\omega)+Ztg(\omega)\rfloor \\ & - I_{i+1}(\omega)\cdot Ztg(\omega) - I_{i\ \ 1}(\omega)\cdot Ztg(\omega) \\ & - \sum_{j=i+1}^{6} I_j(\omega)\cdot Zm_{i,j}(\omega) + \sum_{j=i}^{i\ \ 1} I_j(\omega)\cdot Zm_{i,j}(\omega) \end{aligned} \tag{1}$$

where:

$$\begin{aligned} Zt_i(\omega) &= \frac{Zt(\omega)\cdot Ztt(\omega)}{Zt(\omega)+Ztt(\omega)} \quad \forall i\in\{1,2,4,5,6\} \\ Zt_3(\omega) &= Z_c(\omega) \end{aligned}$$

In matrix form, currents components may be obtained as follows:

$$[V]=[Z]\cdot[I]\Rightarrow[I]=[Z]^{\ 1}[V]$$

3. Spectral response of voltage distribution along the winding

Once currents $I_i(\omega)$ have been computed, turn to ground voltages $V_i(\omega)$ at each node can be easily computed using $Ztg(\omega)$. The result is the spectral response of the voltage distribution along the winding. This is most valuable information, because it allows us to analyse the dielectric response of the insulating material and detect changes therein by comparison with frequency domain spectroscopy (FDS) measurements

4. Prediction of voltage distribution.

With this methodology, it is very easy to predict voltage distribution in the time domain by applying the inverse FFT algorithm.

3 Measurement of electrical parameters

A stator core from a standard induction motor has been used to analyse the internal voltage distribution. As stated in the previous section, it is of great interest to measure the voltages in the first- and last groups of turns because these are the points where electrical stresses are higher, so a new 49 turns coil has been randomly wound and inserted into the stator core with taps at turns#1,#2,#46,#47,#48,#49. With such a 49-turns coil, a fully detailed distributed parameter model with 49 nodes ladder network would be impractical and would require a very high computational effort. So a simplified model has been used instead, with 44 central turns being represented by a single lumped parameters network.

The complete set of electrical parameters in the model can be easily determined with a small number of experimental measurements and some simplifying assumptions. Measurements have been made by means of an impedance analyser (Solartron SI 1260) to obtain real- and imaginary part of each impedance within a 100 Hz–9 MHz frequency range, which would serve to analyse pulse rise times as short as 39 ns (commercially available inverters do not usually have rise times below 100 ns). Figures 2, 3 and 4 show the complete arrangement of the experimental setup.

Due to the limited number of taps along the winding, the general form of the mathematical model has been adapted, gathering the central 44-turns section into a single elementary mesh. This drastically reduces the computational effort when solving the model equations but without any loss of relevant information, because, as stated above, the most interesting regions are the first and the final turns of the coil where wave reflections may appear.

The experimental procedure comprises four types of measurements:

– Measurement of series impedance of a single turn.

The impedance of a single turn ($Zt(\omega)$) consists of an inductance in series with a frequency dependent resistance, to account for the skin effect. In our experiment, measurement is done on a separate turn of the same wire diameter and length placed close to the phase coil, in the slot opening. Turn reactance measurement should be

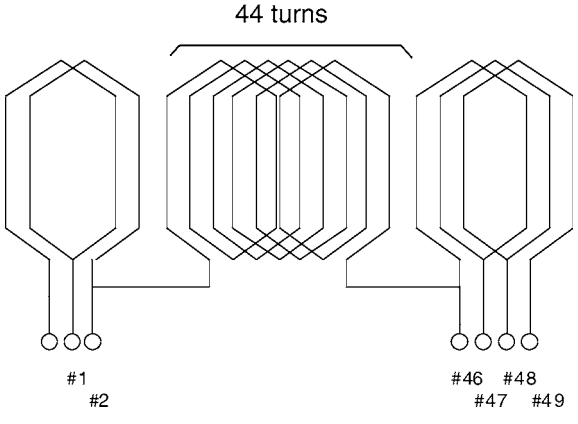

Fig. 2 Actual arrangement of the tested coil

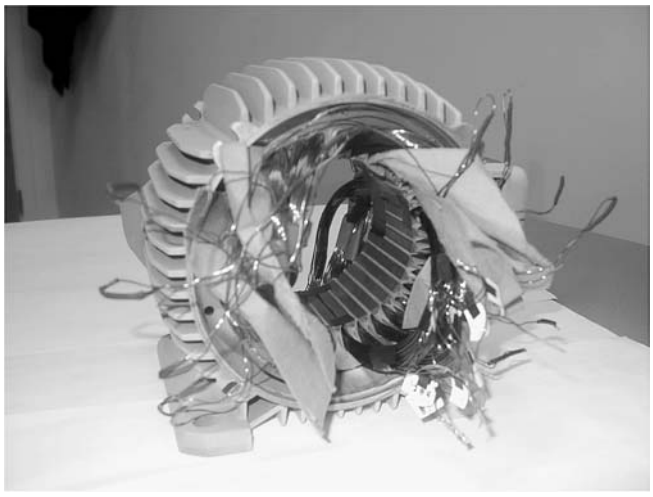

Fig. 3 Motor used in the experiment showing the tapped coil

Fig. 4 General view of the experimental setup

made in order to take into account high frequency magnetic flux penetration into the iron plates. Magnetic saturation seems to have little influence in the initial voltage distribution since relative permeability is not reported as a dominant factor compared to stray capacitances [4]

– Measurement of series impedance of the central section coil.

Series parameters L and R of the central section coil are measured in the same way as above, as a function of frequency. In our experiment, the impedance across the central 44 turns has been directly measured instead.

– Measurement of turn-to-ground capacitance.

In order to account for dielectric losses a parallel R-C network has been used. The measurement procedure involves applying a voltage signal between a single turn and ground, irrespective of its position in the slot. This value is taken as valid for every turn in the whole coil [11].

– Measurement of turn-to-turn capacitance

Also described by a parallel R-C network, the measurement was made between the beginnings of two adjacent turns in the overhang section of the coil. According to many authors [3, 11, 14, 15], only capacitances between consecutive turns have been taken into account.

$$\begin{aligned} Ztt(\omega) &= \quad Z_{k,j}(\omega) \quad \forall k \in \{1,2,47,48,49\}, \ \ \forall j = k-1 \\ \frac{1}{Z_{k,j}(\omega)} &= \quad 0 \quad \forall j < k-1 \end{aligned}$$

These values should be completed by the mutual inductance parameters between two successive turns. This direct measurement is cumbersome, especially on a fully finished motor, so the following approximation has been adopted, according to previously published works [1, 15]:

$$Zm_{ij}(\omega) = j \cdot \omega \cdot M_{ij}$$
$$M_{ij} = k \cdot L_i \cdot L_j,$$

where the constant k takes values usually between 0.7 and 1.0 depending on the physical proximity between turns in the overhang region. Self-inductances L_i and L_j are directly obtained from measurements. The values of the model parameters at different frequencies are included in Table 1.

4 Analysis of voltage distribution in the frequency domain

Once the whole model parameters have been obtained, node voltages can be computed when a 1 pu amplitude, variable frequency ideal source is applied between the coil input terminal and ground. Equation (1) is solved using Matlab. The resulting voltage amplitudes at each winding tap are represented in Fig. 5 as a function of frequency. The effect of full reflection at the open end of the winding can be observed, causing node voltages of up to 2 pu. In this case, as the source is applied directly to the coil input there is no significant voltage overshoot across the first two turns. Very good agreement between results obtained from the theoretical model (Fig. 5a), and experimental measurements (Fig. 5b) can also be observed.

Table 1 Values of model parameters

Frequency	100 Hz	100 kHz	1 MHz
R	2,04E 02 Ω	1,11E 01 Ω	3,85E 01 Ω
L	5.27E 7H	7.17E 7H	9.79E 8H
Rtt	9 MΩ		
Ctt	33.77 pF		
Rtg	9 MΩ		
Ctg	41.87 pF		

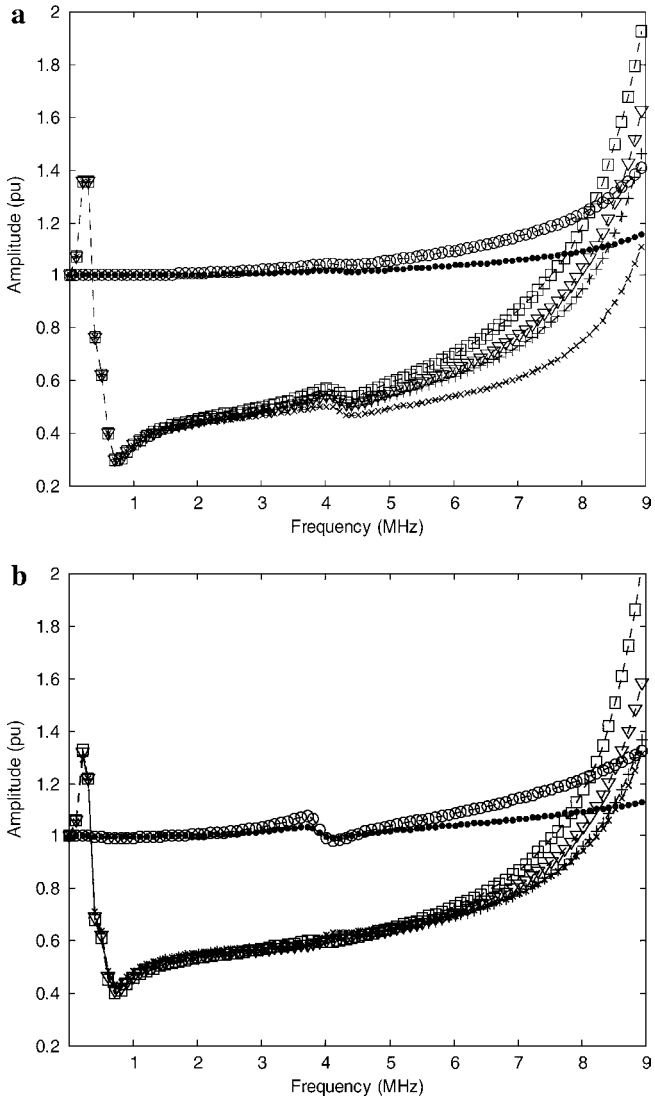

Fig. 5 **a** Voltage amplitude at taps#1(·), #2(*circle*), #46(*x*), #47 (+), #48(*triangle*), #49 (*square*). Theoretical model. **b** Voltage amplitude at taps#1(·), #2(*circle*), #46(*x*), #47(+), #48 (*triangle*), #49 (*square*). Experimental measurements

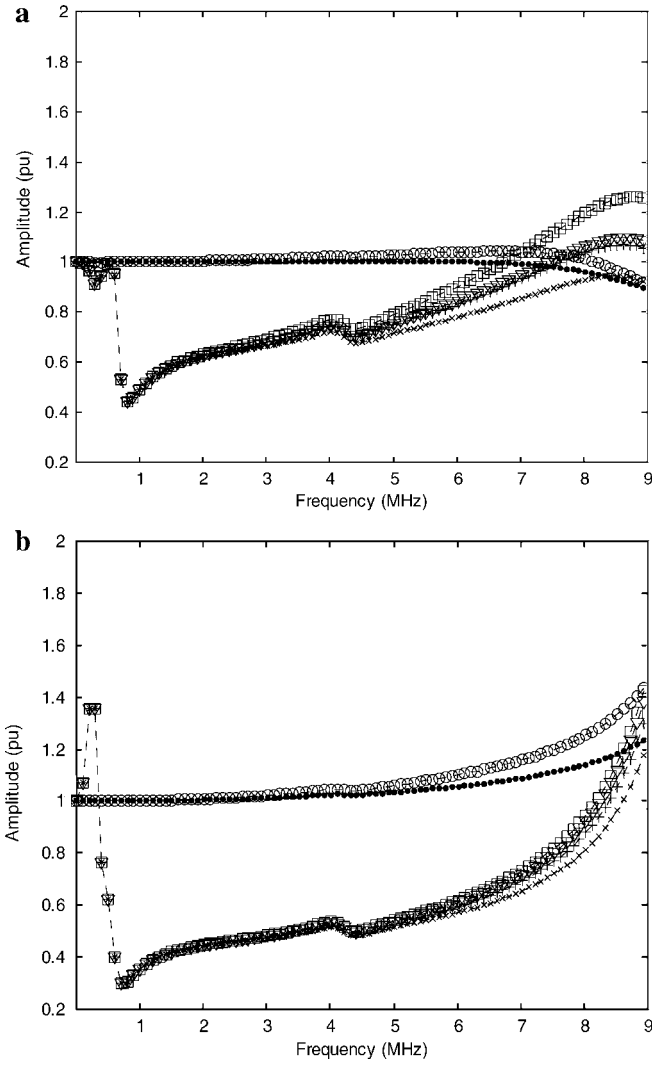

Fig. 6 **a** Theoretical voltage amplitude at taps#1 (·), #2 (*circle*), #46 (*x*), #47(+), #48(*triangle*), #49(*square*), when neglecting loss representing elements. **b** Theoretical voltage amplitude at taps#1 (·), #2 (*circle*), #46 (*x*), #47 (+), #48 (*triangle*), #49(*square*), when neglecting mutual inductances between turns

5 Effect of simplifying assumptions on accuracy

The effect of neglecting some model parameters such as power losses or mutual inductances can be easily observed in Fig. 6. In the first case (Fig. 6a) a considerable mismatch appears between experimental and theoretical values of voltage magnitude as a consequence of neglecting losses in the model. Similar diagrams can be obtained for the voltage phase. Other authors have stated that despite neglecting these losses there is adequate agreement with experimental data [9], nevertheless it is clear from the results presented here that prediction accuracy degrades in the high frequency ranges associated with short pulse rise times. This conclusion is in agreement with some recently published works [6, 11].

Also the effect of neglecting mutual inductances increases model error, as shown in Fig. 6b, although its influence is minor compared with that of loss-representing elements (see Table 2). Mean accumulated absolute errors (both in amplitude and phase) are used to quantify the accuracy of theoretical results when compared with experimental ones. Voltage differences between experimental and theoretical data are averaged for each frequency in all nodes. Final error value is the result of averaging the above values for all nodes.

6 Prediction of voltage distribution in time domain

This prediction capability of the model can be transposed to the time domain by applying an Inverse Fast

Table 2 Mean accumulated absolute errors in amplitude and phase

Model	Amplitude error (V)	Phase error (rad)
Lossless	0,1009	0,4592
Neglecting mutual inductances	0,0803	0,0296
Complete	0,0590	0,0290

Fourier Transform defined by the transfer functions $H_k(\omega)$.

$$V_k(\omega) = H_k(\omega) \cdot V_i(\omega), \tag{2}$$

where $V_k(\omega)$ and $V_i(\omega)$ are the fast Fourier transform of the nodal voltage $v_k\ (t)$ and the input voltage $v_i\ (t)$, respectively. This implies choosing an adequate sampling interval for the theoretical excitation signal, and computing the values of the frequency spectrum coherent with this sampling time ($\Delta t = 55$ ns in our case). In order to get comparable results the chosen excitation signal, applied to the theoretical and experimental transfer functions, is a cuasi-square step impulse with a rise time of 120 ns. The actual signal applied to the experimental setup is very similar in shape, with the same amplitude and approximately the same rise time. Both signals are shown in Fig. 7.

Finally, time domain response to these steep-fronted pulses (Fig. 7a) for all turns $v_k\ (t)\ \forall\ k \in \{1,2,46, 47,48,49\}$ is easily obtained applying inverse fast fourier transform (iFFT) to Eq. 2. The results of voltage distribution along the different taps using both experimental (see Fig. 5b) and theoretical transfer functions (see Fig. 5a) are presented in Fig. 8a, where dotted points (•) represent the output voltage values in the last open-ended #49 turn, computed when the theoretical excitation signal $v_i\ (t)$ is applied to the coil model, and crossed points (x) are the result of applying the i-FFT transformation to the measured transfer functions in the frequency domain. The ultimate comparison is shown in Fig. 8b, representing the directly measured time response of the coil when a real periodic square wave signal (as in Fig. 7b) is applied. Despite the different scales, a very good agreement between both responses can be concluded, with an overshoot of 1.4 pu and a very similar shape.

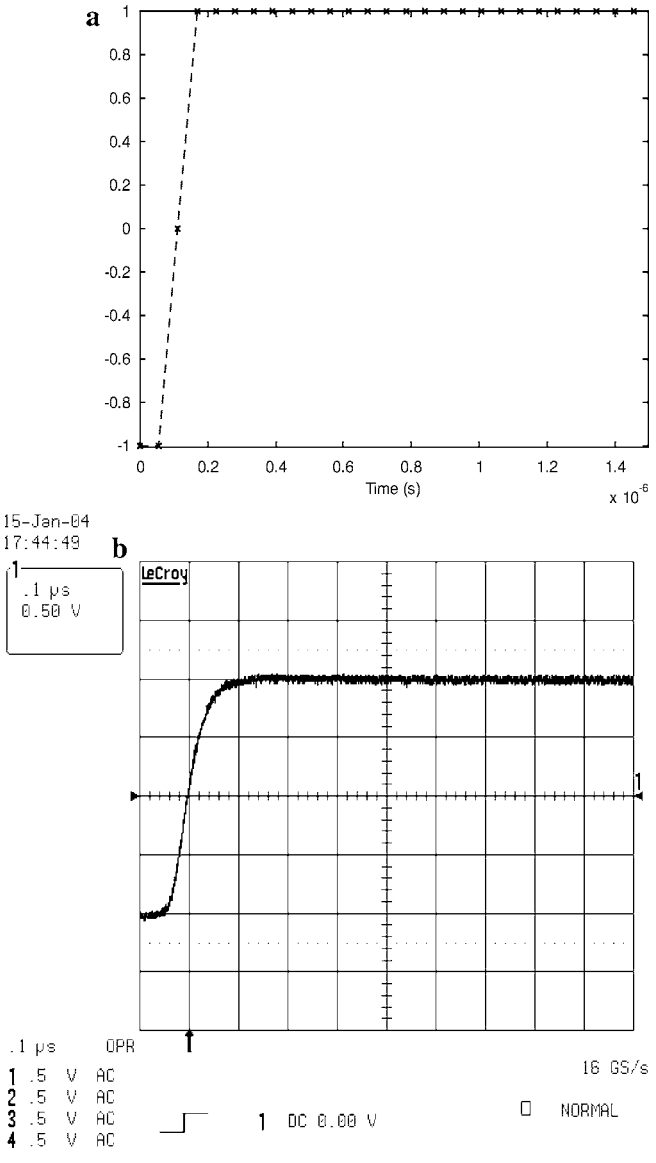

Fig. 7 **a** Theoretical excitation signal. **b** Experimental excitation signal

7 Conclusion

A new model that permits the analysis and prediction of voltage distribution along random windings in low voltage motors fed by PWM sources has been presented in this work. This analytical approach not only allows us to predict turn to ground voltages, but also turn to turn voltage distribution along the winding, while other previously published works deal only with voltage prediction between coils. The model has been formulated and developed in the frequency domain, and its parameters can be easily determined by a well-defined and reduced set of measurements. The model, whose ability to predict nodal voltages up to a frequency of 9 MHz has been proved, can also predict voltage distribution in time domain when an inverse FFT transform is performed, subject to several constraints in the choice of sampling time and number of points. In addition to the information that can be obtained in the time domain (overvoltage amplitude of both turn-to-turn and turn-to-ground values), the model also holds important information related to the frequency response of the dielectric materials which can be of great value for ageing studies.

As can be seen from these results, model ability for voltage distribution prediction is proved to be equally accurate for time domain studies too. In fact, direct

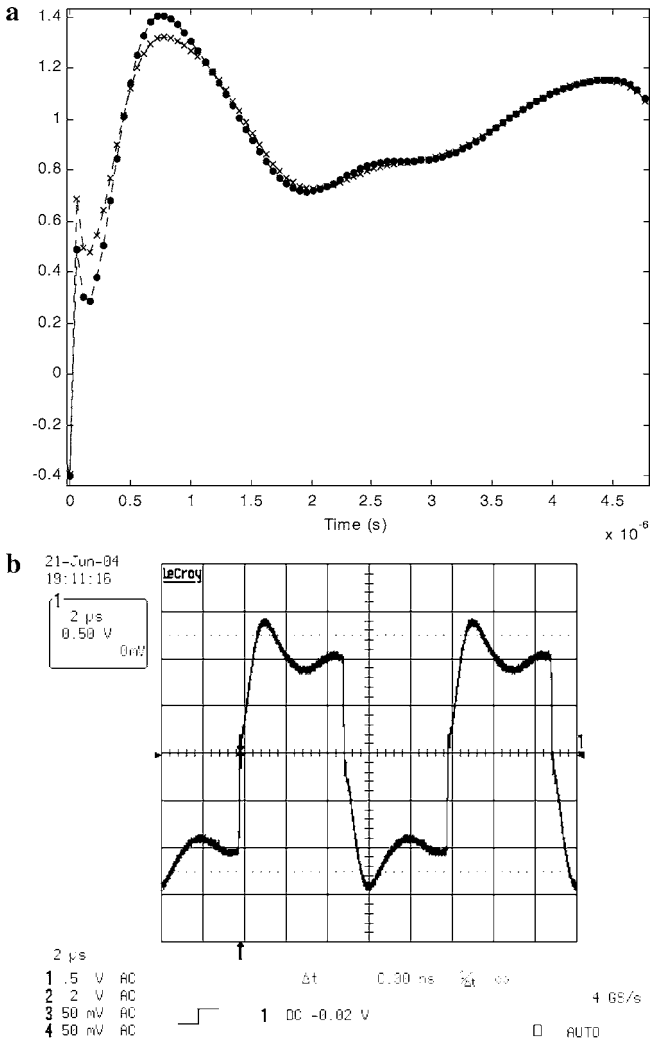

Fig. 8 **a** Voltage time domain results obtained from theoretical (•) and experimental (*x*) transfer functions. **b** Voltage time domain direct measurements

measurements were also made on the winding taps by applying a real low voltage pulse signal having a similar rise time as that used in prediction. Predicted values of voltage propagation along the windings show a very close agreement with experimentally measured ones.

Acknowledgements This research has been supported by the Spanish Science and Technology Ministry under contract MAT 2002 03210, and the Madrid Regional Government under the Ini tiative for Regional R&D Laboratory Network. Tests have been made in the High Voltage Research and Tests Laboratory of Universidad Carlos III de Madrid (LINEALT).

References

1. Gubbala L, Von Jouanne A, Enjeti P, Singh C, Toliyat H (1995) Voltage distribution in the windings of an AC motor subjected to high dv/dt PWM voltages. Power Electronics Specialists Conference
2. Melfi M, Sung AMJ, Bell S, Skibinski G (1998) Effect of surge voltage risetime on the insulation of low voltage machines fed by PWM converters. IEEE Trans Industry Applications
3. Toliyat HA, Suresh G, Abur A (1999) Estimation of voltage distribution on the inverter fed random wound induction motor windings supplied through feeder cable. IEEE Trans Energy Conversion
4. Al Ghubari FH, Von Jouanne A, Wallace AK (2001) The ef fects of PWM inverters on the winding voltage distribution in induction motors. Electric Power Components Syst
5. Bidan P, Lebey T, Neascu C (2003) Development of a new off line test procedure for low voltage rotating machines fed by adjustable speed drives (ASD). IEEE Trans Dielectrics Elec trical Insulation
6. Oyegoke BS (2000) A comparative analysis of methods for calculating the transient voltage distribution within the stator winding of an electric machine subjected to steep fronted surge. Electrical Eng
7. Mbaye A, Bellomo JP, Lebey T, Oraison JM, Peltier F (1997) Electrical stresses applied to stator insulation in low voltage induction motors fed by PWM drives. IEE Proc Electric Power Applications
8. Kaufhold M, Börner G, Eberhardt M, Speck J (1996) Failure mechanism of the interturn insulation of low voltage electric machines fed by pulse controlled inverters. IEEE Electrical Insulation Mag
9. Wright MT, Yang SJ, McLeay K (1983) General theory of fast fronted interturn voltage distribution in electrical machine windings, IEE Proc
10. Guardado JL, Cornick KJ (1989) A computer model for cal culating steep fronted surge distribution in machine windings. IEEE Trans on Energy Conversion
11. Martínez JM, Amarís H, Sanz J (2003) Steep fronted transients in inverter fed motors. In: XIIIth international symposium on high voltage engineering
12. Neacsu C (2002) Contribution à L'Etude des Défaillances Statoriques des Machines Asynchrones : Mise au Point et Réalisation d'un Test Non Destructif de Fin de Fabrication. These du grade de Docteur de L'Universite Paul Sabatier
13. Humiston T, Pillay P (2004) Experimental setup for the mea surement of surge propagation in induction machines. IEEE Trans Energy Conversion
14. Lupo G, Petrarca C, Vitelli M, Tucci V (2002) Multiconductor transmision line analysis of steep front surges in machine windings. IEEE Trans Dielectrics Electrical Insulation
15. Jianru W, Hongchi L, Huanjun Y (2002) Voltage distribution in stator windings of the motor driven by PWM inverter. Proceedings of Power System Technology Conference